MRS Advances © 2016 Materials Research Society
DOI: 10.1557/adv.2016.652

Pulsed Electrodeposition of Tin Electrocatalysts onto Gas Diffusion Layers for Carbon Dioxide Reduction to Formate

Sujat Sen,[1] Brian Skinn,[2] Tim Hall,[2] Maria Inman,[2] E. Jennings Taylor[2] and Fikile R. Brushett[1]

[1]Department of Chemical Engineering, Massachusetts Institute of Technology, Cambridge, MA, 02139, USA
[2]Faraday Technology, Inc., Englewood, OH, 45315, USA

ABSTRACT

This paper discusses a pulse electroplating method for developing tin (Sn)-decorated gas diffusion electrodes (GDEs) for the electrochemical conversion of carbon dioxide (CO_2) to formate. The pulse-plated Sn electrodes achieved current densities up to 388 mA/cm^2, more than two-fold greater than conventionally prepared electrodes (150 mA/cm^2), both at a formate selectivity of 80%. Optical and microscopic analyses indicate improvements in deposition parameters could further enhance performance by reducing the catalyst particle size.

INTRODUCTION

The development of energy efficient carbon dioxide (CO_2) electroreduction processes would simultaneously curb anthropogenic CO_2 emissions and provide sustainable pathways for the generation of fuels and chemicals. While significant efforts have focused on heterogeneous CO_2 electroreduction to various products, to date, few studies have demonstrated both high current efficiency (> 60 %) and high current densities (> 150 - 200 mA/cm^2) simultaneously [1-5]. A key challenge in the development of active, selective, and stable electrocatalysts is scaling performance nanomaterials to appropriate electrode structures, which augment catalytic activity by maximizing utilization, facilitating reactant/product transport, and minimizing undesirable side reactions. The electroreduction of CO_2 to formic acid (FA) or its salts such as sodium formate, is attractive due to the low charge requirement (i.e., 2 electrons per FA), the liquid-state product, and the high product selectivity on a number of low-cost catalytic materials [6]. FA has a range of commercial uses including silage, textiles, leather tanning, pharmaceuticals, crop-protection, and latex processing [7]. It may also find use as a fuel for direct liquid fuel cells [8]. While a number of metals can be used for this reaction, tin (Sn) is of particular interest due to its high selectivity, low cost, and lack of toxicity [6].

The performance of Sn-based electrodes is largely dependent on the ability to efficiently deliver CO_2 to the catalyst sites. Prior reports have demonstrated electroreduction of CO_2 to FA on Sn catalysts at varying current efficiencies (10-95%) on disk electrodes, metal meshes, and gas diffusion electrodes (GDEs) which operate at a range of currents (10-200 mA/cm^2) depending on modes of CO_2 transport [6, 7, 9-13]. In addition, recent work has shown that product selectivity decreases with increasing catalyst loading likely due to mass transport losses within a thick catalyst layer [10]. Thus, there is a need to investigate new approaches to electrode development that maximize performance in terms of product generation rate, selectivity, and catalyst utilization. Conventionally, a GDE is prepared by depositing an ink consisting of Sn catalyst particles, ionomer, and carrier solvents onto gas diffusion layer (GDL) via painting,

spraying, or doctor-blading [14]. In general, the gas diffusion media, either carbon paper or carbon cloth, consists of two layers: a Teflon-treated fibrous backing layer and microporous layer (MPL), which consists of a mixture of carbon particles and Teflon (Figure 1a). The electrocatalyst is coated on the MPL side of the GDL which interfaces with a liquid or solid electrolyte. As depicted in Figure 1b, this approach limits the electroreduction of CO_2 due to 1) low catalyst specific surface area due to the relatively large particle size (here, ≥150 nm), and 2) unutilized Sn catalyst particles within the ionomer but not in electrical contact with the carbon in the MPL. Fabrication technologies able to produce smaller (< 10 nm) particles can alleviate the former aspect, but can do little to address the latter. Previous work directed towards platinum (Pt) catalyst utilization in polymer electrolyte fuel cell GDEs demonstrated a novel "electrocatalyzation" (EC) approach (Figure 1c) that used pulse and pulse reverse electrodeposition to obtain highly dispersed and uniform Pt catalyst nanoparticles (~5 nm) [15-17]. Moreover, since the catalyst was electroplated through an ionomer layer on to the bare carbon MPL, the formed nanoparticles were inherently in both electronic and ionic contact within the GDE and, consequently, utilization was enhanced. Specifically, for the oxygen reduction reaction, the electrodeposited catalyst exhibited equivalent performance at 0.05 mg/cm^2 loading compared to a conventionally prepared GDE with a loading of 0.5 mg/cm^2 [17].

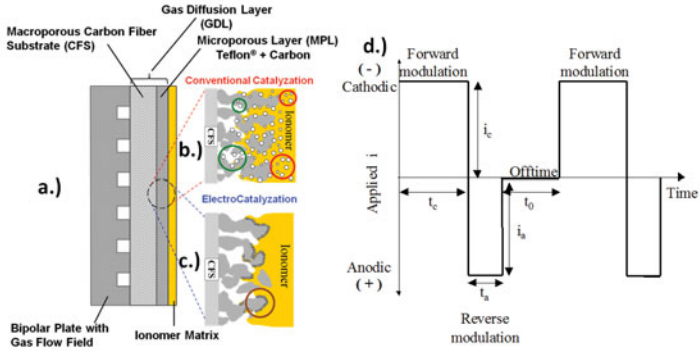

Figure 1. Schematic representation of (a) the layers of a GDE, (b) conventional catalyzation with regions of catalyst with no ionic access (green circles) and no electronic access (red circles); (c) electrocatalyzation with simultaneous electronic and ionic access (brown circle), (d) generic waveform used with pulse and pulse-reverse sequences.

The EC process utilizes pulse and pulse reverse waveforms to enhance control over the surface chemistry and mass transfer dynamics of electrochemical processes. Figure 1d shows an example of a typical waveform, consisting of a cathodic (forward) pulse followed by an anodic (reverse) pulse and a relaxation period (off-time). The cathodic peak current (i_c), cathodic on-time (t_c), anodic peak current (i_a), anodic on-time (t_a), and the relaxation-time (t_o) are individual variables for process control. In pulse and pulse reverse processes, there are unlimited combinations of peak current densities, duty cycles, and frequencies to obtain a given electrodeposition rate, allowing precise control of the process and consequently the properties of the deposit specific to an application. In conventional direct current (DC) electrochemical

processing, the current is turned on and held for the duration of the process. By interrupting this constant current, as in the EC process, one may achieve results not possible with conventional DC techniques. In the case of electroplating, these include control of alloy composition, nucleation densities, and microstructure, as well as the use of simplified plating chemistries.

Here we investigate the electrocatalytic performance of novel Sn catalysts electrodeposited directly onto the MPL of a GDL after the application of an ionomer layer, as shown in Figure 1c. Our goal is to improve the Sn catalyst utilization by eliminating particles that are not in electronic contact with the carbonaceous GDL. The EC samples are benchmarked against commercial Sn catalysts (150 nm), mixed with ionomer and spray-coated onto the GDL. By using pulse/pulse reverse electrodeposition, we aim to enhance nucleation versus growth and thereby increase the catalyst specific surface area by decreasing the particle size (<< 150 nm).

EXPERIMENT

Materials

Sodium carbonate (99.999%, Sigma Aldrich), LIQUion 1100 EW (Ion Power Inc., 15% w/w), tin nanoparticles (150 nm, Sigma Aldrich), methanesulfonic acid (70% w/w, Atotech USA Inc.), stannous methanesulfonate (300 g-Sn/L, Atotech), Triton X-100 (Sigma), H_2 (99.9%, Ultra High Purity 5.0, Airgas) and CO_2 (99.99%, Research Grade 5.0, Airgas), platinum on Vulcan XC-72 (20 wt.%, Fuel Cell Store), Nafion 117 membrane (Fuel Cell Store), and gas diffusion layers (Sigracet GDL 39BC, Ion Power Inc.) were used as received.

Preparation of conventional gas diffusion electrodes

Sigracet 39 BC GDLs were used as the substrate in this study. The cathodes (Sn-150) were air-brushed whereas the anode (Pt on Vulcan) was brush painted onto the MPL of the GDL. For the air-brushed cathodes, catalyst inks were prepared by combining and sonicating 10 mg Sn catalyst, 6.9 μL LIQUion, 400 μL Millipore water, and 400 μL isopropyl alcohol. For the brush painted anodes, catalyst inks were prepared as per previously reported procedures [14]. Typical loading of the cathodes and anodes were ca. 0.35 mg/cm^2 and 1 mg/cm^2, respectively, as determined by weighing the sample before and after deposition.

Pre-treatment of gas diffusion layers with ionomer for electrodeposition

Two methods were tested for application of ionomer to GDL samples prior to Sn electroplating, brush painting and buoyant floating. In all cases, the stock ionomer dispersion was diluted from 15% (as supplied) to 4.77%, 1.49%, and 0.46% w/w with isopropanol to examine the effect of ionomer concentration. GDL ionomer loadings were measured by weighing each GDL sample before and after ionomer application, after drying overnight in air. Loadings between 0.11 and 7.56 mg/cm^2 were obtained across the two methods and dispersion concentrations used. For brush painting, ionomer dispersions were painted onto GDL samples with a fine-tip art brush. For the floating method, GDL samples were floated with MPL side down on ionomer dispersion contained in a small glass vessel for varying lengths of time (3-20

min); in some cases samples were floated for multiple time intervals with set drying periods between each.

Pulsed electrodeposition of tin onto ionomer-treated gas diffusion layers

Catalyst electrodeposition was performed in a custom cell equipped with patented flow hardware for enhanced flow uniformity (Figure 2a-c) [18-21]. A custom holder was fabricated to hold 4 cm × 4 cm GDLs for electrodeposition. The cell was charged with a tin-methanesulfonate (Sn-MSA) electrodeposition bath (240 mL L^{-1} of 70% w/w MSA, plus 107 g L^{-1} Sn^{2+}) with continuous circulation at 7.57 L/min as measured by an inline rotameter. In most tests, 300 mg/L Triton X-100 was included in the plating bath to enhance surface wetting. GDLs were mounted in the custom holder and inserted directly into the electrodeposition cell. A DC, forward-pulse, or pulse-reverse waveform was applied under current control for a defined period of time. The actual voltage and current responses at the cell were measured by oscilloscope (Tektronix, Salem, OR) to confirm the fidelity of the applied waveform and to calculate the actual net cathodic charge passed in each test. After plating, the Sn-coated GDEs were removed from the cell, gently rinsed with deionized water, photographed, and left to dry overnight in a fume hood. Catalyst loadings on the GDLs were determined by weighing the sample before and after deposition using an analytical balance (Scientech SA 210) with a precision of 0.1 mg.

Electrolysis experiments & product quantification

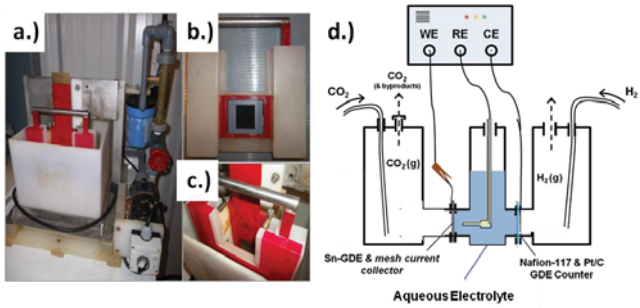

Figure 2. Photographs of the cell used for Sn electrodeposition on GDL: (a) full view including pump, piping, and flowmeter; (b) GDL sample holder; (c) holder mounted for electrodeposition, with a sacrificial tin sheet anode and (d) W-cell for electrochemical testing of Sn GDEs.

Electrolysis experiments were performed in a three compartment cell (a W-cell) schematized in Figure 2d. Electrolysis was performed using an aqueous electrolyte of 0.5 M Na_2CO_3 and 0.5 M Na_2SO_4 under potentiostatic conditions using a VSP-300 Biologic potentiostat. The counter electrode was a Pt-coated GDE hot pressed on to a Nafion 117 membrane at 130 °C and 0.34 MPa (50 psi) for 5 min [22]. CO_2 and H_2 were delivered to the working and counter GDEs at 20 mL/min throughout the experiment. All potentials reported herein are referenced to the Ag/AgCl electrode (+197 mV vs. SHE). Liquid phase products were quantified using solvent suppressed 1D ^{1}H NMR (400 MHz, Bruker Avance) as per previously reported procedures [23].

DISCUSSION

Pulsed electrodeposition of tin onto the gas diffusion layer

We are developing an electrocatalyzation (EC) technique to deposit Sn catalyst particles selectively only in electrode regions with both ionic and electronic accessibility as depicted in Figure 1c. In this technique, we coat the bare carbon MPL of a commercially available GDL with Nafion by either painting or float-coating methods. This is followed by electrodeposition of Sn particles through the Nafion layer onto the MPL from a commercial plating bath. Figure 3a shows good linearity of the ionomer loading as a function of the number of painting cycles. For the floating procedure, the ionomer loading was found to be fairly insensitive to the float time, but strongly dependent on the concentration of the dispersion as shown in Figure 3b. Sn loadings between 0.05 and 2.32 mg/cm^2 were obtained across the electrodeposition conditions examined.

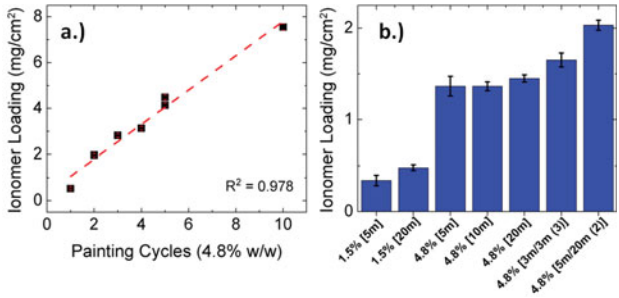

Figure 3. (a) Ionomer loading vs. painting cycles with a 4.8% w/w solution and (b) ionomer loading vs. different floating parameters (c [f/d (#)]; c = dispersion ionomer concentration (% w/w); f = floating time (m); d = drying time between floats (m); # = number of times floated).

Physical characterization of tin-loaded gas diffusion electrodes

In Figure 4, we present optical images of the electrocatalyzed (EC) and conventional (Sn-150) electrocatalysts. The spray coated Sn-150 sample (Figure 4a), used as a benchmark in this study, appeared visibly uniform, whereas the EC samples (Figure 4b, c) appeared to be more heterogeneous with pockets of localized deposits.

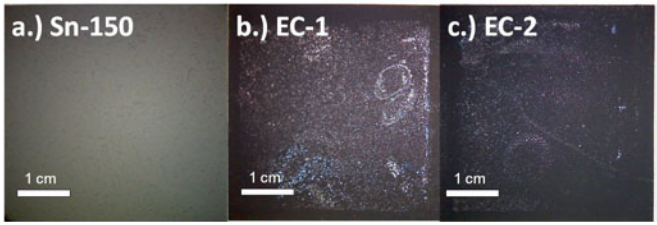

Figure 4. Optical images of Sn-coated GDEs (a) via spray coating; (b, c) via EC.

Figure 5 shows the SEM images of the EC and Sn-150 samples. An average particle size of 100-200 nm is visible for the conventional GDE, whereas the EC sample shows agglomerates of 1-20 µm. Future efforts will focus on enhancing nucleation versus growth through optimization of the electrodeposition waveforms and thereby decreasing the Sn catalyst particle size (<< 150 nm), as previously demonstrated for Pt [15-17]. A Zeiss Merlin High Resolution SEM was used to image the cross section of the EC sample (Figure 5c, f), confirming that the electrodeposited Sn was confined to a thickness of ~10 µm on the MPL and does not penetrate into the bulk of the GDL.

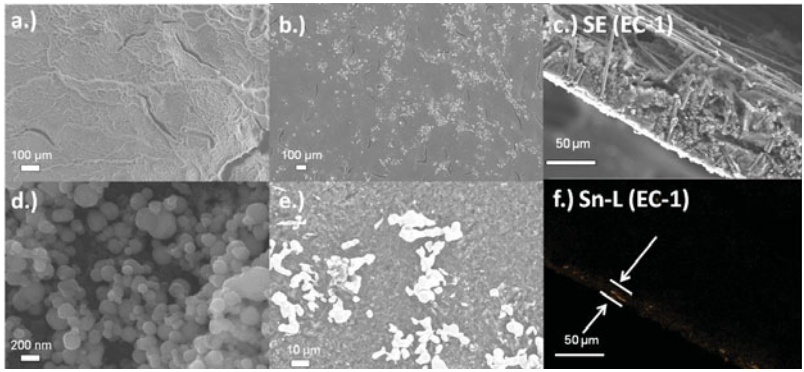

Figure 5. SEM images of Sn-coated GDEs (a, d) via spray coating; (b, e) via EC; (c) the cross sectional view of an EC GDE and (f) associated EDX mapping at the Sn-L edge.

Electrochemical characterization of tin loaded gas diffusion electrodes

The polarization curves shown in Figure 6a compare the CO_2 reduction performance of the EC and conventional electrodes. For a given potential and at comparable mass loadings, the EC samples achieve higher current density than the conventional samples. At higher mass loadings, the EC sample continues to perform at a comparable level, suggesting possible saturation in current response as a function of catalyst loading. To note, the preliminary nature of the data in the present study prohibits meaningful interpretation of the differing polarization of EC-1 and EC-2. Future work will attempt to correlate electrode behavior with the upstream electrodeposition conditions and with downstream electrocatalytic performance.

To investigate the steady-state performance of these samples, longer duration electrolysis experiments were performed. Figure 6b shows measured current densities and formate selectivities for the present GDEs, as well as selected literature values [7, 9, 10, 12, 13] chosen for comparison due to the use of a tin electrocatalyst and gas-phase delivery of CO_2. Moreover, all these studies utilize an electrolyte of comparable ionic strength (1M or greater), allowing for a good comparison of current densities. Specific values shown represent the highest current density reported in these studies. For both EC samples, we observe a higher absolute and partial

current density (to formate) as compared both to the benchmark (Sn-150) and to notable prior reports.

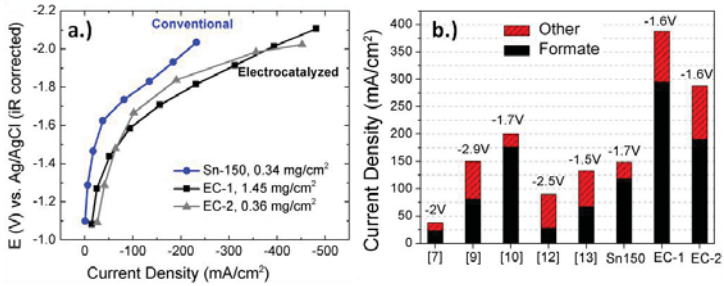

Figure 6. (a) Polarization curves of Sn-150 and EC GDEs based on a 1 min chronoamperometric measurement (b) Plot of current densities obtained during the 1 h electrolysis test of the same GDEs compared to prior literature. All potentials are reported vs. Ag/AgCl electrode.

To note, there is a discrepancy in the current densities between Figures 6a and 6b, which arises from the nature of the measurement technique employed: the former uses the current density measured at 1 min, whereas the latter uses the average stabilized value of current density from an hour-long experiment. The initial (1 min) current density, comparable to that reported in figure 6a, gradually increases, attaining a stable value within the first hour, which is reported in Figure 6b. This phenomenon is attributed to a "break in" process of the gas diffusion electrode due to gradual wetting, which in turn allows for progressively increasing access to the catalyst matrix and hence increasing current density. Similar behavior has been observed in previous literature [7, 10, 24]. No appreciable decrease in current density was observed over the course of the 1h electrolysis.

CONCLUSIONS

The electrocatalyzation process based on pulsed waveforms was used to successfully electrodeposit Sn directly onto Nafion-coated GDLs. These EC electrodes were subsequently tested for their activity in the electroreduction of CO_2 to formate, achieving a maximum current density of 388 mA/cm^2 and formate selectivity of 80%, which outperforms recent literature reports. We hypothesize that the observed enhancement in performance arises from the intimate contact of the catalyst particles to both carbon in the microporous layer and ionomer simultaneously. This ensures both electronic and ionic access to the catalyst, which are necessary for the conversion of CO_2 to formate via a proton coupled electron transfer (PCET) process. This is in contrast to GDEs prepared by conventional methods, where a substantial fraction of the loaded catalyst is not in simultaneous electronic and ionic contact, and thus exhibits appreciably lower performance. We further hypothesize that additional performance enhancement may be attainable by dramatic reductions of the catalyst particle size, below 10 nm. We anticipate optimization of the pulsed waveform conditions will enable reductions on this order of magnitude, based upon prior experience with Pt electrocatalysts [15-17]. Future studies will focus on tailoring the pretreatments, deposition parameters, and bath conditions to optimize the performance and durability of these novel electrodes.

ACKNOWLEDGMENTS

The authors acknowledge the financial support of DOE SBIR Contract #DE-SC0015173. This work made use of the MRSEC Shared Experimental Facilities at MIT, supported by the National Science Foundation under award number DMR-1419807.

REFERENCES

1. I. Merino-Garcia, E. Alvarez-Guerra, J. Albo, A. Irabien, Chem. Eng. J., 305, 104-120 (2016).
2. E. Irtem, T. Andreu, A. Parra, M.D. Hernandez-Alonso, S. Garcia-Rodriguez, J.M. Riesco-Garcia, G. Penelas-Perez, J.R. Morante, J. Mater. Chem. A, 4, 13582-13588 (2016).
3. D. Pletcher, Electrochem. Commun., 61, 97-101 (2015) .
4. A. M. Appel et al., Chem. Reviews, 113, 6621-6658 (2013).
5. S. Verma, B. Kim, H.-R.M. Jhong, S. Ma, P. J. A. Kenis, ChemSusChem, 9, 1972-1979 (2016).
6. Y. Hori, H. Wakebe, T. Tsukamoto, O. Koga, Electrochim. Acta, 39, 1833-1839 (1994).
7. A.S. Agarwal, Y. Zhai, D. Hill, N. Sridhar, ChemSusChem, 4, 1301-1310 (2011).
8. A.K. Singh, S. Singh, A. Kumar, Catal. Sci. Technol. 6, 12-40 (2016).
9. A. Del Castillo, M. Alvarez-Guerra, J. Solla-Gullón, A. Sáez, V. Montiel, A. Irabien, Appl. Energy, 157, 165-173 (2015).
10. D. Kopljar, A. Inan, P. Vindayer, N. Wagner, E. Klemm, J. Appl. Electrochem., 44, 1107-1116 (2014).
11. G.K.S. Prakash, F.A. Viva, G.A. Olah, J. Power Sources, 223, 68-73 (2013).
12. A. Del Castillo, M. Alvarez-Guerra, A. Irabien, AIChE Journal, 60, 3557-3564 (2014).
13. H. Li, C. Oloman, J. Appl. Electrochem., 35, 955 (2005).
14. H.-R.M. Jhong, F.R. Brushett, P.J.A. Kenis, Adv. Energy Mater., 3, 589-599 (2013).
15. M. E. Inman, E.J. Taylor, U.S. Patent No. 6,080,504, (27 June 2000).
16. N .R.K. Vilambi Reddy, E. B. Anderson, E.J. Taylor, U.S. Patent No. 5,084,144, 28 Jan 1992).
17. E.J. Taylor, E.B. Anderson, N.R.K. Vilambi, J. Electrochem. Soc., 139, L45-L46 (1992).
18. L. E. Gebhart, J. J. Sun, P. O. Miller, E. J. Taylor, U.S. Patent No. 8,329,006 (11 December 2012).
19. L. E. Gebhart, E. J. Taylor, U.S. Patent No. 8,226,804 (24 July 2012).
20. L. E. Gebhart, E. J. Taylor, U.S. Patent No. 7,947,161 (24 May 2011).
21. L. E. Gebhart, J. J. Sun, P. O. Miller, E. J. Taylor, U.S. Patent No. 7,553,401 (30 June 2009).
22. J. Wu, F.G. Risalvato, S. Ma, X.-D. Zhou, J. Mater. Chem. A, 2, 1647-1651 (2014).
23. S. Sen, D. Liu, G.T.R. Palmore, ACS Catal., 4, 3091-3095 (2014).
24. D. Kopljar, A. Inan, P. Vindayer, N. Wagner, E. Klemm, Chem. Eng. Technol., 39, 2042-2050 (2016).